International Journal of Mechanical, Industrial and Aerospace Sciences
ISSN: 2517-9950
Vol:8, No:7, 2014

# Interval Type-2 Fuzzy Vibration Control of an ERF Embedded Smart Structure

Chih-Jer Lin, Chun-Ying Lee, Ying Liu, Chiang-Ho Cheng

***Abstract*—**The main objective of this article is to present the semi-active vibration control using an electro-rheological fluid embedded sandwich structure for a cantilever beam. ER fluid is a smart material, which cause the suspended particles polarize and connect each other to form chain. The stiffness and damping coefficients of the ER fluid can be changed in 10 micro seconds; therefore, ERF is suitable to become the material embedded in the tunable vibration absorber to become a smart absorber. For the ERF smart material embedded structure, the fuzzy control law depends on the experimental expert database and the proposed self-tuning strategy. The electric field is controlled by a CRIO embedded system to implement the real application. This study investigates the different performances using the Type-1 fuzzy and interval Type-2 fuzzy controllers. The Interval type-2 fuzzy control is used to improve the modeling uncertainties for this ERF embedded shock absorber. The self-tuning vibration controllers using Type-1 and Interval Type-2 fuzzy law are implemented to the shock absorber system. Based on the resulting performance, Internal Type-2 fuzzy is better than the traditional Type-1 fuzzy control for this vibration control system.

***Keywords*—**Electro-Rheological Fluid, Semi-active vibration control, shock absorber, type 2 fuzzy control.

## I. INTRODUCTION

RECENTLY, smart materials have been inspired and designed in living applications. For vibration control, smart materials are very suitable to be a tunable vibration absorber (TVA) due to their varied physical phenomena. Smart materials use various controllable material properties to achieve the vibration control. For example, shape memory alloys (SMA) can change its material properties based on temperature; piezo-electrical ceramics can produce the force or displacement based on the piezoelectric effect; magnetic-rheological fluids (MRF) and electro-rheological fluids (ERF) can change the stiffness and damping coefficients of the fluids based on magnetic-rheological and electro-rheological properties. Electro-rheological fluids are smart controllable fluids with suspensions of extremely fine non-conducting particles (up to 50 micrometers diameter) in an electrically insulating fluid. The apparent viscosity of ERFs can change reversibly in response to an electric field. The apparent viscosity of these fluids can change reversibly by an order of up to 100,000 in response to an electric field. A typical ERF can change from a liquid to a gel with response times of milliseconds. Generally, the ER effect is also called the Winslow effect, because this effect was first discovered and reported by Willis Winslow, who obtained a US patent on the effect in 1947 [1]. ERF have drawn many studies on the theoretical modeling and applications since the discovery of ERF by Winslow in 1940's. The ERF changes from a Newton fluid to a forming chain-like structure as an enough high electric field is applied to the fluid. The gel is called a Bingham plastic, which is a viscoplastic material. The Bingham plastic usually behaves as a rigid body at a low stress. When the applied stress is enough high, it will flow and behave as a viscous fluid. However, when the applied electric field is removed, the ERF behaves as a Newton fluid with response times of milliseconds. These reversible and controllable rheological properties of ERFs make them attractive for applications in devices such as clutches, valves, shock absorbers, and vibration dampers [2]. ER fluids have been studied in vibration controls of structure by many researchers using various control strategies for decades. Choi et al. derived an empirical model for predicting the vibration characteristics responding to electrical field and studied the vibration properties for hollow cantilevered beams filled with ER fluids [3]. Yalcintas et al. investigated the semi-active control of ER adaptive beams and illustrated the capabilities theoretically and experimentally [4]. Choi et al. investigated the active vibration control and the active vibration characteristics of hollow cantilevered beams embedded with ER fluids [5]. Rahn and Joshi (1998) designed a feedback control system to control the vibration of the cantilevered ER beam [6]. Wei et al. investigated the feasibility of applying ER fluids to the vibration control of rotating flexible beams [7].

The dynamic vibration absorber was first invented by Frahm tin 1911 [8] and the traditional dynamic vibration absorber is an auxiliary mass-spring system which is tuned the attached position to cease the vibration motion. Applying dynamic vibration absorbers is a cheap and easy-to-maintain solution for suppressing vibration in vibrating systems with harmonic excitation, but vibration can be eliminated only at the attachment point while amplification of vibration may occur in other parts of the beam [9]–[11]. Other ideas of tunable vibration absorbers (TVA) were developed by many researches various for various applications [12]-[16]. Different from the DVA, a TVA is a smart structure with tunable stiffness and damping coefficients to play a tunable absorber which is

Chih-Jer Lin and Ying Liu are with Graduate Institute of Automation Technology, National Taipei University of Technology, Taipei 10608, Taiwan (886-2-2771-2171 ext. 4328; fax: 886-2-2711-1401; e-mail: cjlin@ ntut.edu.tw).

Chun-Ying Lee is now with the Department of Mechanical Engineering, National Taipei University of Technology, Taipei 10608, Taiwan (e-mail: leech@ ntut.edu.tw).

Chiang-Ho Cheng is with the Department of Mechanical and Automation Engineering, University of Dayeh, Dacun, Changhua, Taiwan, (e-mail: chcheng@mail.dyu.edu.tw).

attached to a structure. To make the smart structure have controllable stiffness and damping properties, many smart materials have been used, such as viscoelastic solid, shape memory alloys, piezoelectric materials, ER fluids, MR fluids and elastomers. The mechanisms of the variable stiffness can be achieved via the change in geometry or adjustment in the material properties [12]-[15]. ER fluids change from Newtonian flow to Bingham plastic as the applied electric field is applied, because the electric field makes the suspended particles polarized and connected with each other to form chain. Therefore, the viscosity and the yield stress of the ER fluid increases as soon as the electric field is applied. The stiffness and damping properties of a sandwich beam embedded with ER fluids can be easily varied and controlled. Lin et al. studied an embedded ERF sandwich as a TVA for a vibration control [16]. However, the accurate parameters of ERF models are generally difficult to obtain and the modeling uncertainties of the TVA always exists. To improve the performance of the TVA, a Type2-fuzzy semi-active controller is studied to deal with the modelling uncertainties in this study.

Type-2 fuzzy sets and systems have become very popular during the past decade. Even though Zadeh proposed type-2 fuzzy sets in 1976, focus on type-1 fuzzy sets is much more than on type-2 fuzzy sets [17]. This changed in the latter part of the 1990s as a result of Mendel and his student's works on type-2 fuzzy sets and systems [18]. Recently, more and more researchers around the world are studying about type-2 fuzzy sets and systems for various applications [19]-[27]. In fact, Zadeh proposed more sophisticated kinds of fuzzy sets, the first of which he called a *type-2 fuzzy set* [17]. Type-2 fuzzy sets are used to handle the uncertainties of the type-1 fuzzy set, because the membership function of a type-1 fuzzy set has no uncertainty associated with it. A type-2 fuzzy set lets us incorporate uncertainty about the membership function into fuzzy set theory. However, if there was no uncertainty, a type-2 fuzzy set would reduce to a type-1 fuzzy set. Different from the type-1 fuzzy set, the membership function of a general type-2 fuzzy set is three-dimensional, where the third dimension is the value of the membership function at each point on its two-dimensional domain that is called its footprint of uncertainty (FOU). To reduce the complicated computation of type-2 fuzzy set, an interval type-2 fuzzy set was proposed. For the interval type-2 fuzzy set, the third-dimension value is the same everywhere. As a result, the third dimension is ignored and only the FOU is used to describe it. Type-2 fuzzy sets are very wide applicability recently in rule-based fuzzy logic systems (FLSs), because they let uncertainties be modeled by them whereas such uncertainties cannot be modeled by type-1 fuzzy sets [27].

This paper is organized as follows. Section II describes the fabrication of the ERF sandwich beam and the characteristic measurement of the ERF embedded TVA (ERTVA) in the frequency domain. The frequency response is measured to establish the fuzzy expert database for the vibration controller. Section III describes the vibration control architecture using the ERTVA to suppress the vibration of a cantilevered beam structure. Based on the experimental results, Type-1 and Type-2 fuzzy controllers are proposed to accomplish the semi-active vibration control. In Section IV, the real-time implementation is performed to validate the proposed controller using NI compact RIO. Finally, Section V draws conclusions.

## II. The System Setup

### A. Fabrication of ER Sandwich Beam

A ER sandwich beam is designed and made as the same as our previous research in [16]. The top and bottom plates of sandwich beam are made of aluminum with the thickness of 0.3mm. The ER dam has four edges made of rubber and the ER fluid is confined in the volume between the rubber edges and aluminum plates. The ER fluid consists of two components: corn starch and silicon oil (KF-96-20cs), where the weight fraction of the corn-starch suspensions is almost 45%~50%. The two aluminum plates also play as the electrodes of the applied electrical field. An acrylic pad is used as the rigidity for the clamped side, which can be connected to the other structure as a TVA.

### B. Measurement of the ER Sandwich Beam's Characteristics

The measurement of the ER sandwich beam's characteristics is also the same with our previous research [16]. Fig. 1 depicts a schematic diagram of the experimental setup for measuring the dynamic characteristics of the ER beam specimen. An electromagnetic vibration shaker (LDS PA500L) provides the exciting force to the clamped side of the ER beam. Two non-contacting eddy-current displacement probe (Keyence AH-416) are used to measure the deflection of the input excitation and the ER beam's free end. A high-voltage power amplifier provides the electrical field for the electrodes of the aluminum face-plates during the test. A dynamic signal analyzer (HP 35665A) is used to analyze the dynamic characteristics of the ER beam as the different applied electric fields. The dynamic signal analyzer provides an actuating signal for the shaker in the form of a swept sine wave at the frequency from 0 to 200 Hz and then the input and output measured time response signals were fed to the dynamic signal analyzer. The frequency response can be obtained using fast Fourier transform (FFT) in HP 35665A for the ERF embedded beam. The same experimental steps were repeated at varying electrical field from 0 to 2 ($kV/mm$) in 0.25 ($kV/mm$) increments. Fig. 2 shows the relationship between the frequency response and the corresponding electric field of the ER sandwich beam. The peak values of each curve represent the natural frequencies of the ER sandwich beam. Fig. 3 illustrates the effect of electric field strength at the frequency of the first mode and the first mode frequency increases as the strength of the applied electrical field increases. Based on the results in Figs. 2-3, the material properties of ER sandwich beam can be controlled by changing the strength of the applied electric field. Therefore, the ER sandwich beam can become a TVA to incorporate with a main structure to suppress vibration. For the first mode, the amplitude of the resonant frequency decreases as the applied electric field increases as shown in Fig. 3. Therefore, using the half-power point method can obtain the relation between the damping ratios of the whole system with respect to the applied electric field as shown in Table I.

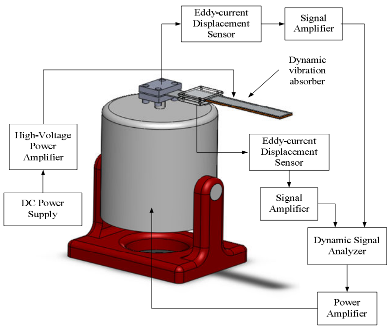


Fig. 1 Schematic diagram of semi-active vibration control architecture for a structure using the ER sandwich TVA

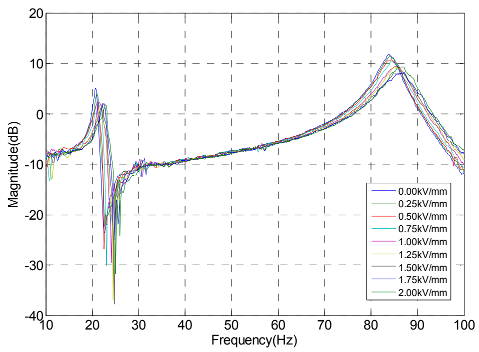


Fig. 2 The relationship between the frequency response and the corresponding electric field of the ER sandwich beam

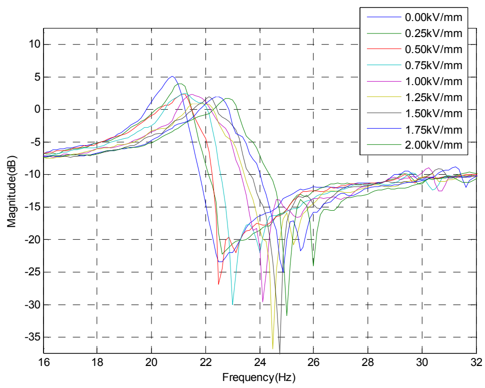


Fig. 3 Effect of electric field on the ER sandwich beam

TABLE I
THE RELATION BETWEEN THE DAMPING RATIO, THE 1ST MODE FREQUENCY AND THE APPLIED ELECTRIC FIELD

| E(kV/mm) | f(Hz) | Amplitude(dB) | Damping ratio($\zeta$) |
|---|---|---|---|
| 0 | 20.625 | 5.0541 | 0.0235 |
| 0.25 | 21 | 3.9032 | 0.0233 |
| 0.5 | 21 | 2.3085 | 0.0342 |
| 0.75 | 21.125 | 2.4819 | 0.0401 |
| 1 | 21.375 | 2.2658 | 0.0322 |
| 1.25 | 21.625 | 0.9183 | 0.0383 |
| 1.5 | 22 | 1.9752 | 0.0295 |
| 1.75 | 22.375 | 1.9526 | 0.0298 |
| 2 | 22.75 | 1.7164 | 0.0380 |

## III. FUZZY SEMI-ACTIVE CONTROLLER DESIGN

To understand that the stiffness and energy dissipation characteristics of the ERF beam with respect to the applied electric field, an immediate selection is to choose the optimal electrical field based on the field-dependent frequency responses in Fig. 3. If an electrical field could minimize the envelopes of the amplitude at the excitation frequency bandwidths, the vibration of the structure would be suppressed as soon as possible. Therefore, numerous studies are designed to be performed to capture the characteristics of the ER sandwich beam. After that the fuzzy controller for attenuating the undesired vibration for the ERF cantilevered beam can be established using the frequency-dependent control strategy [16]. The switching algorithm of the controlled electric field can be designed according to the mapping between the frequency response and the applied electric field.

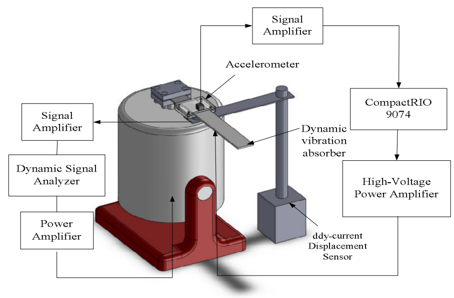


Fig. 4 Schematic diagram of semi-active vibration control architecture for a structure using the ERTVA

### *A. Vibration Control Design Using the ERTVA*

Fig. 4 shows a proposed schematic diagram of semi-active vibration control architecture for a structure using the ERTVA [16]. The accelerometer (PCB 333B32) is used to measure the acceleration of the main structure at the free end and this signal is fed back to the real-time controller (cRIO-9074), which implements the proposed fuzzy controllers to produce the control signal. After that, the high-voltage power amplifier (Trek 609A) is used to amplify the control signal for producing the electric field to the ERF. The dynamic signal analyzer (HP 35665A) is used to capture the signal from the eddy-current probe to compare the time responses the open loop system with the closed loop system with the proposed vibration controller. Fig. 5 shows the

International Journal of Mechanical, Industrial and Aerospace Sciences
ISSN: 2517-9950
Vol:8, No:7, 2014

experimental testing setup of the ERTVA using the proposed semi-active vibration control architecture.

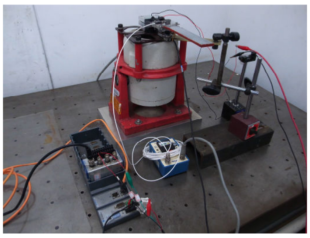

Fig. 5 The experimental testing setup of the ERTVA

To establish the fuzzy rule base for the vibration controller, some experiments should be performed with respect to different frequencies and various amplitudes at first. Table II shows the experimental results of the structure for applying the different applied electric field (0, 0.5, 1, 1.5, 2 (kV/mm)) on the ER-TVA for the excitation with the specified amplitudes at the frequency of 10 Hz. Tables III-VII shows the experimental results of the structure for applying the different applied electric field (0, 0.5, 1, 1.5, 2 (kV/mm)) on the ER-TVA for the excitation at the frequencies of 15, 20, 25, 30, 35 (Hz). In these tables, the bold fonts represent the optimal choice at the specified excitation, because the root-mean-square (RMS) value of the acceleration for the main structure is minimized. The RMS value of the acceleration is obtained as follows.

$$a_{rms} = \sqrt{\frac{1}{T}\int_{T_1}^{T_2} a^2 dt} \quad (3)$$

where $a_{rms}$ is the root-mean-square value (RMS) of the acceleration, $T_1$ and $T_2$ are the initial and final time, and $T$ $T=T_2-T_1$.

TABLE II
THE ACCERROMETER OUTPUT OF THE STRUCTURE FOR APPLYING THE DIFFERENT APPLIED ELECTRIC FIELD ON THE ERTVA FOR THE EXCITATION AT FREQUENCY OF 10 HZ

| Sinusoidal excitation at 10Hz | | Shaker input ($mV_{pk}$) | | |
|---|---|---|---|---|
| Accelerometer output ($mV_{rms}$) | | 30 | 40 | 50 |
| Electric field (kV/mm) | 0 | 2.73 | 3.69 | 5.54 |
| | 0.5 | 2.13 | **2.61** | 4.14 |
| | 1 | 1.82 | 2.75 | 3.93 |
| | 1.5 | 1.75 | 2.87 | 3.77 |
| | 2 | **1.64** | 2.66 | **3.45** |

TABLE III
THE ACCERROMETER OUTPUT OF THE STRUCTURE FOR APPLYING THE DIFFERENT APPLIED ELECTRIC FIELD ON THE ERTVA FOR THE EXCITATION AT FREQUENCY OF 15HZ

| Sinusoidal excitation at 15Hz | | Shaker input ($mV_{pk}$) | | |
|---|---|---|---|---|
| Accelerometer output ($mV_{rms}$) | | 30 | 40 | 50 |
| Electric field (kV/mm) | 0 | **4.15** | 6.32 | 7.93 |
| | 0.5 | 4.33 | **6.15** | **7.26** |
| | 1 | 5.03 | 6.53 | 7.75 |
| | 1.5 | 5.09 | 7.15 | 8.46 |
| | 2 | 4.96 | 7.06 | 8.39 |

TABLE IV
THE ACCERROMETER OUTPUT OF THE STRUCTURE FOR APPLYING THE DIFFERENT APPLIED ELECTRIC FIELD ON THE ERTVA FOR THE EXCITATION AT FREQUENCY OF 20HZ

| Sinusoidal excitation at 20Hz | | Shaker input ($mV_{pk}$) | | |
|---|---|---|---|---|
| Accelerometer output ($mV_{rms}$) | | 30 | 40 | 50 |
| Electric field (kV/mm) | 0 | 9.12 | 14.97 | 19.64 |
| | 0.5 | **7.69** | 11.35 | 14.88 |
| | 1 | 8.06 | **10.91** | **13.36** |
| | 1.5 | 8.24 | 12.65 | 14.54 |
| | 2 | 8.87 | 12.53 | 15.78 |

TABLE V
THE ACCERROMETER OUTPUT OF THE STRUCTURE FOR APPLYING THE DIFFERENT APPLIED ELECTRIC FIELD ON THE ERTVA FOR THE EXCITATION AT FREQUENCY OF 25HZ

| Sinusoidal excitation at 25Hz | | Shaker input ($mV_{pk}$) | | |
|---|---|---|---|---|
| Accelerometer output ($mV_{rms}$) | | 30 | 40 | 50 |
| Electric field (kV/mm) | 0 | 12.67 | 17.73 | 24.51 |
| | 0.5 | 12.83 | 18.04 | 24.09 |
| | 1 | 12.06 | 17.35 | 23.43 |
| | 1.5 | 10.75 | 16.09 | 21.87 |
| | 2 | **9.33** | **14.25** | **19.83** |

TABLE VI
THE ACCERROMETER OUTPUT OF THE STRUCTURE FOR APPLYING THE DIFFERENT APPLIED ELECTRIC FIELD ON THE ERTVA FOR THE EXCITATION AT FREQUENCY OF 30HZ

| Sinusoidal excitation at 30Hz | | Shaker input ($mV_{pk}$) | | |
|---|---|---|---|---|
| Accelerometer output ($mV_{rms}$) | | 30 | 40 | 50 |
| Electric field (kV/mm) | 0 | 22.67 | 29.97 | 37.55 |
| | 0.5 | 20.22 | 27.66 | 35.44 |
| | 1 | 19.85 | 26.85 | 34.68 |
| | 1.5 | 19.53 | 26.42 | 33.94 |
| | 2 | **18.47** | **25.58** | **33.15** |

TABLE VII
THE ACCERROMETER OUTPUT OF THE STRUCTURE FOR APPLYING THE DIFFERENT APPLIED ELECTRIC FIELD ON THE ERTVA FOR THE EXCITATION AT FREQUENCY OF 35HZ

| Sinusoidal excitation at 35Hz | | Shaker input ($mV_{pk}$) | | |
|---|---|---|---|---|
| Accelerometer output ($mV_{rms}$) | | 30 | 40 | 50 |
| Electric field (kV/mm) | 0 | 38.83 | 51.57 | 64.66 |
| | 0.5 | 33.94 | 46.47 | 59.09 |
| | 1 | 31.49 | 43.35 | 55.42 |
| | 1.5 | **29.35** | **40.57** | **52.15** |
| | 2 | 30.46 | 41.62 | 53.54 |

The fuzzy rules can be established by using the above experimental results in Tables II-XII. Fig. 6 shows the block diagram of the fuzzy control with two inputs and one output. The first input of the fuzzy controller is the root-mean-square (RMS) value of the acceleration, which provides the information about the amplitude of the vibration and the second input of the fuzzy controller is the vibration frequency, which is obtained using FFT value of the accelerometer on the structure. In this study, Type-1 and Type-2 fuzzy controllers are proposed to build the fuzzy mapping between the excitation and the optimal electric field to the ERTVA.

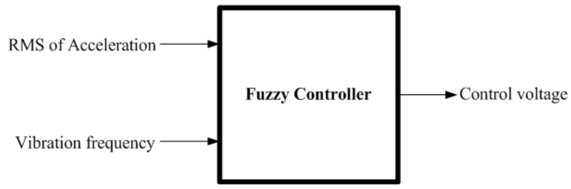


Fig. 6 The structure of the proposed fuzzy controller [16]

### *B. Type-1 Fuzzy Controller Design*

According to the look-up table in Tables II-VII, the type-1 fuzzy rules can be determined as shown in Table VIII, where the inputs are the windowed RMS value of the acceleration and the frequency of the excitation, which can be obtained using the FFT from the acceleration signal. There are four membership functions, which involves of VS (very small), S (small), M (medium), and B (big) as shown in Figs. 7-8. For the control output of the Type-1 fuzzy controller, four membership functions are shown in Fig. 9, where the larger number means the larger electric field to the ERTVA. Therefore, the control output of the fuzzy controller is produced using D/A module NI 9263 and this signal is amplified through the high voltage power amplifier (Trek 609A) to control the stiffness of the TVA to suppress the vibration of the main structure. Fig. 10 shows the input-output mapping relation of the proposed fuzzy controller.

TABLE VIII
RULES OF THE TYPE-1 FUZZY CONTROLLER

| *Freq.* \ *RMS of acceleration* | VS | S | M | B |
|---|---|---|---|---|
| VS | M | S | S | S |
| S | S | M | B | VB |
| M | M | M | VB | VB |
| B | VB | B | B | B |

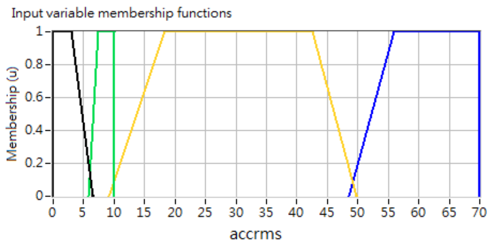


Fig. 7 Membership functions for the first input

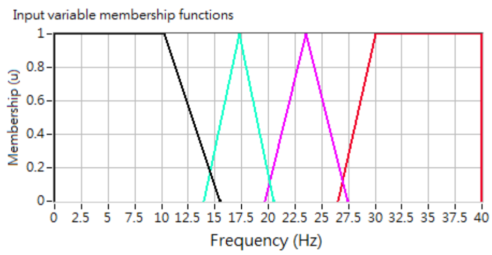


Fig. 8 Type-1 fuzzy Membership functions for the second input

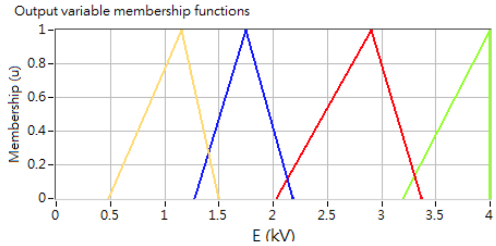


Fig. 9 Type-1 fuzzy Membership functions for the output

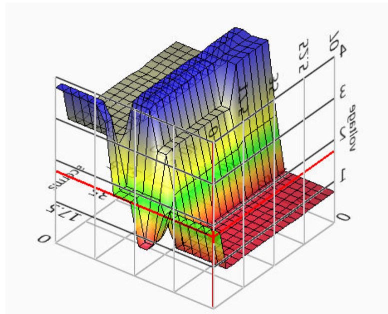

Fig. 10 The input-output mapping relation of the Type-1 fuzzy controller

### *C. Interval Type-2 Fuzzy Controller Design*

An interval type-2 Fuzzy Logic System (FLS) is studied for vibration control in presence of system unmodeling measurement noises and external disturbances. A type-2 fuzzy system has a similar structure with type-1 fuzzy, but one of the major differences can be seen in the rule base part, where a type-2 rule base has antecedents and consequents using Type-2 Fuzzy Sets. In this study, a Gaussian function with a known standard deviation is considered and a uniform weighting is assumed to represent a footprint of uncertainty as shaded in Figs. 11-12. Because of using such a uniform weighting, it is usually called an Interval Type-2 Fuzzy Set (IT2FS) [25]. For the IT2FS, a type-reducer is needed to convert to a type-1 fuzzy set before defuzzification is carried out as shown in Fig. 13. To obtain the output of the IT2FS, two fuzzy rules are needed as shown in Tables XI-X. Fig. 14 shows the inference operation to obtain the output by using the following equations.

$$\bar{f} = \prod_{i=1}^{N} \bar{u}_{\tilde{A}}(x_i) \tag{1}$$

$$\underline{f} = \prod_{i=1}^{N} \underline{u}_{\tilde{A}}(x_i) \tag{2}$$

where N is the number of the inputs.

After obtaining the inference output, we used the type-reducer and defuzzifier to obtain the input-output relation as shown in Fig. 15.

International Journal of Mechanical, Industrial and Aerospace Sciences
ISSN: 2517-9950
Vol:8, No:7, 2014

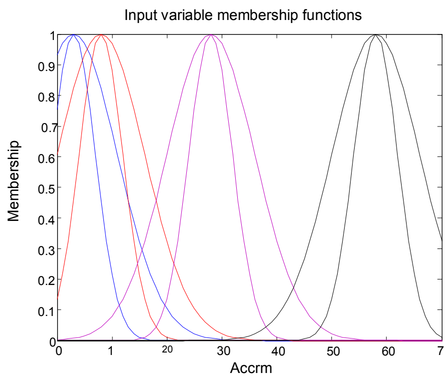


Fig. 11 Type-2 fuzzy Membership function for the first input

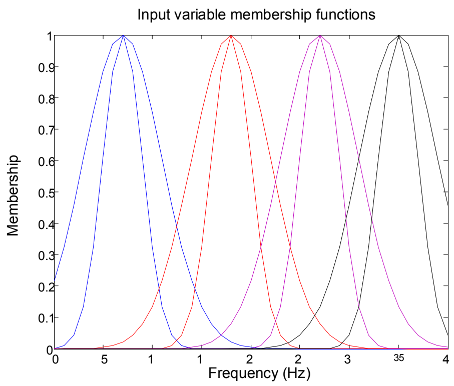


Fig. 12 Type-2 fuzzy Membership function for the second input

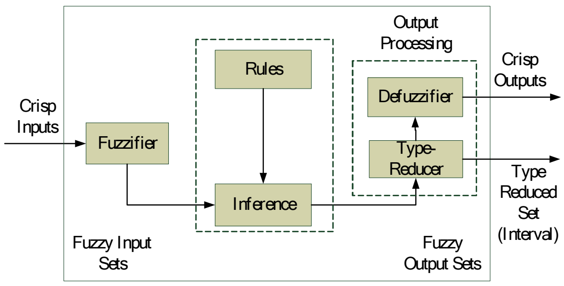


Fig. 13 Main structure of Type-2 fuzzy

TABLE IX

RIGHT FUZZY RULE

| Frequency \ $Acc_{rms}$ | VS | S | M | B |
|---|---|---|---|---|
| VS | M | S | S | S |
| S | S | M | B | VB |
| M | M | M | VB | VB |
| B | VB | B | B | B |

TABLE X

LEFT FUZZY RULE

| Frequency \ $Acc_{rms}$ | VS | S | M | B |
|---|---|---|---|---|
| VS | VB | VB | VB | VB |
| S | B | Z | Z | Z |
| M | Z | Z | Z | Z |
| B | S | S | M | VB |

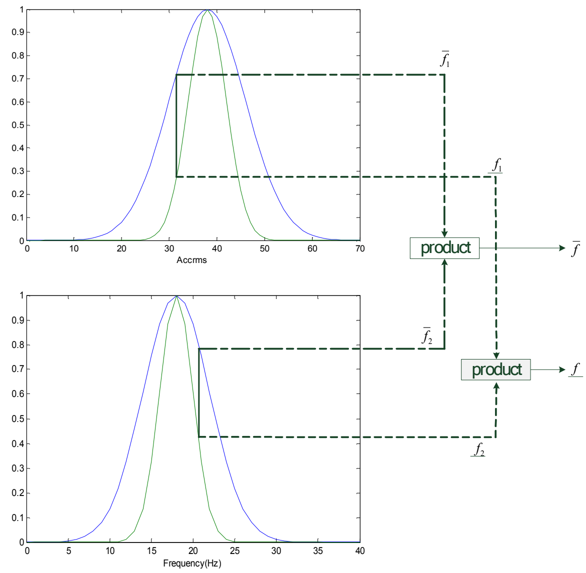


Fig. 14 The inference operation of Type-2 fuzzy

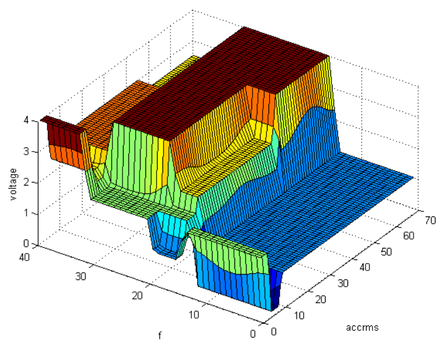


Fig. 15 The input-output mapping relation of the Type-2 fuzzy controller

## IV. Experimental Results and Discussion

The excitation signals at the frequencies from 15 to 33 Hz are inputted to the shaker to make the structure vibrate and the comparisons between the responses of the type-1 fuzzy controller and the ones of the proposed controller using the IT2FS are summarized in Table XI. Based on the experimental results, the proposed IT2FS controller is better than the type-1 fuzzy controller among the bandwidth of 23~33 Hz. Both the proposed fuzzy controllers (type-1 and type-2) using the ERTVA show vibration suppression at the frequencies between 23 and 33 Hz. However, the ERTVA cannot produce any reduction for the vibration appears at the frequencies 15 and 18 Hz at the frequency of 13Hz, because the structure dynamic is dominant at the frequency under 20Hz. Fig. 3 can explain the above experimental results.

TABLE XI
THE VIBRATION SUPPRESSION RATE USING THE FUZZY CONTROLLERS

| Frequency | Type-1 fuzzy suppression rate | Type-2 fuzzy suppression rate |
|---|---|---|
| 15Hz | 0.00% | 0.00% |
| 18Hz | 0.00% | 0.00% |
| 23Hz | 15.39% | 17.60% |
| 25Hz | 8.29% | 8.96% |
| 27Hz | 7.47% | 9.95% |
| 29Hz | 8.97% | 9.97% |
| 31Hz | 9.65% | 12.34% |
| 33Hz | 12.46% | 13.17% |

## V. CONCLUSIONS

A semi-active fuzzy controller using an ERTVA is presented for the structure's vibration reduction. To implement the proposed fuzzy controller, the fuzzy rules are determined based on the windowed RMS acceleration for specified frequencies and amplitudes. Because there are uncertainties in modelling of the nonlinear characteristics of ERTVA, the proposed IT2FS shows the better performance than the type-1 fuzzy controller. To establish the consistency of the simulation and real-time experimental results, the proposed fuzzy controllers are implemented in real time using the NI CompactRIO. The experimental results verified the effectiveness of the proposed controller using the IT2FS.

## ACKNOWLEDGMENT

The authors would like to thank the National Science Council of the Republic of China, Taiwan, for financially supporting this research under Contract No. NSC 102-2221-E-027 -024.

## REFERENCES

[1] W. M. Winslow, "Induced Fibration of Suspensions," *Journal of Applied Physics*, vol. 20, 1949, pp.1137-1140.
[2] R. S. Stanway, J. L. Sproston, A. K. El Wahed, "Applications of electro-rheological fluids in vibration control: A survey," *Smart Mater. Struct.*, vol. 5, 1996, pp.464-482.
[3] S. B. Choi, Y. K. Park, M. S. Suh, "Elastodynamic characteristics of hollow cantilever beams containing an electro-rheological fluid: Experimental results," *AIAA J.*, vol. 32, 1992, pp.438-440.
[4] M. Yalcintas, J. Pl Coulter, D. L. Don, "Structural modeling and optimal control of electro-rheological material based adaptive beams," *Smart Mater. Struct.*, vol. 4, 1995, pp.207-214..
[5] S. B. Choi, Y. K. Park, C. C. Cheong, "Active vibration control of intelligent composite laminate structures incorporating an electro-rheological fluid," *J. Intell. Mater. Syst. Structures*, vol. 7, 1996, pp.411-419.
[6] C. D. Rahn, S. Joshi, "Modeling and control of an electro-rheological sandwich beam," *J. Vib. Acoust.*, vol. 120, 1998, pp.221-227.
[7] K. X. Wei, G. Meng, W. M. Zhang, "Vibration characteristics of a rotating beam filled with electrorheological fluid," *J. Intell. Mater. Syst. Structures*, vol. 18, 2007, pp.1165-1173.
[8] H. Frahm, "Device for damping vibrations of bodies," US patent no. 989958, 1911.
[9] B.G. Korenev, L.M. Reznikov, "Dynamic Vibration Absorbers, Theory and Technical Applications," Wiley, New York, 1993.
[10] J.P. Den Hartog, "Mechanical Vibrations," Dover Publications Inc., 1985.
[11] J.B. Hunt, "Dynamic Vibration Absorbers," Mechanical Engineering Publications Ltd., 1979.
[12] M. J. Brennan, "Some recent developments in adaptive tuned vibration absorbers/neutralizers," *Shock and Vibration*, vol. 13, 2006, pp. 531–543.
[13] L. Kela, P. Vahaoja, "Recent studies of adaptive tuned vibration absorbers/neutralizers," *Applied Mechanics Reviews*, vol. 62, 2009, pp. 060801-1–060801-9.
[14] A. K. Ghorbani-Tanha, M. Rahimian, A. Noorzad, "A novel semiactive variable stiffness device and its application in a new semiactive tuned vibration absorber," *J. Engineering Mechanics*, vol. 137, 2011, pp. 390–399.
[15] C. Y. Lee, C. C. Chen, T. H. Yang, C. J. Lin, "Structural vibration control using a tunable hybrid shape memory material vibration absorber," *J. Intell. Mater. Syst. Structures,* vol. 23, 2012, pp. 1725-1734.
[16] C. J. Lin, C. Y. Lee, C. H. Cheng, and G. F Chen, "Vibration Control of a Cantilever Beam Using a Tunable Vibration Absorber Embedded with ER Fluids," *International Journal of Mechanical, Industrial Science and Engineering*, Vol. 7 No. 7, 2013, pp. 152-158.
[17] L. A. Zadeh, "The concept of a linguistic variable and its application to approximate reasoning-I," Inf. Sci., vol. 8, 1975, pp.199-249.
[18] J. M. Mendel, *Uncertain Rule-Based Fuzzy Logic Systems: Introduction and New Directions*, Prentice-Hall, Upper-Saddle River, NJ, 2001.
[19] Z. Kovacic, M. Balenovic and S. Bogdan, "Sensitivity based self learning fuzzy logic control for a servo system," *IEEE Control Syst. Mag.*, vol. 18 (3), 1998, pp. 41-51.
[20] H. Lee, M. Tomizuka, "Robust adaptive control using a universal approximator for SISO nonlinear systems," *IEEE Trans. Fuzzy Syst.*, vol. 8 (1), 2000, pp. 95-106.
[21] J. S. Wang, C.S.G. Lee, "Self-adaptive neuro-fuzzy inference systems for classification application," *IEEE Trans. Fuzzy Syst.*, vol. 10 (6), 2002, pp. 790-802.
[22] N. Golea, A. Golea and K. Benmahammed, "Fuzzy model reference adaptive control," *IEEE Transactions on Fuzzy Systems*, vol. 10 (4), 2002, pp. 436-444.
[23] M. Hojati, S. Gazor, "Hybrid adaptive fuzzy identification and control of nonlinear systems," *IEEE Trans. Fuzzy Syst.*, vol. 10 (2), 2002, pp. 198-210.
[24] J. M. Mendel, "Fuzzy Sets for Words: a New Beginning," *Proc. IEEE FUZZ Conference*, St. Louis, MO, May 26–28, 2003, pp. 37–42.
[25] J. M. Mendel, "Computing derivatives in interval type-2 fuzzy logic systems," *IEEE Trans. Fuzzy Syst.* Vol. 12 (1), 2004, pp. 84-98.
[26] C. H. Wang, C. S. Cheng, C. T. Lee, "Dynamical optimal training for interval type-2 fuzzy neural network (T2FNN)." *IEEE Trans. Syst. Man Cybern. Part B*, vol. 34 (3): 1462-1477. 2004.
[27] J. M. Mendel, "Type-2 Fuzzy Sets and Systems: an Overview," *IEEE Computational Intelligence Magazine*, vol. 2, 2007, pp. 20-29.